World Academy of Science, Engineering and Technology
International Journal of Bioengineering and Life Sciences
Vol:16, No:9, 2022

rRNA Maturation Genes (*KRR1* and *PWP2*) in *Saccharomyces cerevisiae* Inhibited by Silver Nanoparticles

Anjali Haloi, Debabrata Das

Abstract**—**Silver nanoparticles inhibit a wide variety of microorganisms. The mechanism of inhibition is not entirely known although it is recognized to be concentration dependent and associated with the disruption of membrane permeability. Data on differential gene expression as a response to nanoparticles could provide insights into the mechanism of this inhibitory effect. Silver nanoparticles were synthesized in yeast growth media using a modification of the Creighton method and characterized with UV-Vis spectrophotometry, transmission electron microscopy (TEM), and X-ray diffraction (XRD). In yeasts grown in the presence of silver nanoparticles, we observed that at concentrations below the minimum inhibitory concentration (MIC) of 48.51 µg/ml, the total RNA content was steady while the cellular protein content declined rapidly. The analysis of the expression levels of *KRR1* and *PWP2*, two important genes involved in rRNA maturation in yeasts, showed up to 258 and 42-fold decreases, respectively, compared to that of control samples. Whether silver nanoparticles have an adverse effect on ribosome assembly and function could be an area of further investigation.

Keywords**—**Ag NP, yeast, qRT-PCR, *KRR1*, *PWP2*.

I. Introduction

SILVER nanoparticles, due to ease of synthesis and wide applicability, are amongst the most ubiquitous manufactured nanoparticles. The use of silver nanoparticles (Ag NPs) as a potent antimicrobial agent is well documented [1]. However, the mechanism(s) of these inhibitory effects are not fully known. Most studies have indicated an interaction of nanoparticles with the cellular membrane and subsequent deformities therein leading to changes in permeability and cell death [2]-[4]. It has also been suggested that nanoparticles will tend to react with other sulfur-containing proteins in the interior of the cell, as well as with phosphorus-containing compounds such as DNA [5]. This interaction will affect physiological processes such as the respiratory chain and cell division finally causing the death of the cell [6]. Ag NPs interact with a wide range of molecular processes within microorganisms resulting in a range of effects from the inhibition of growth, loss of infectivity, to cell death which depends on shape [7], size [8], concentration of Ag NPs, and the sensitivity of the microbial species to silver [9]. It has been suggested that negatively charged cell membrane is attracted to the positively charged Ag^+ ion of nanoparticles, hence the charge of Ag NPs is vital for its antimicrobial activity [10]. The concentration of Ag NPs, associated with pit formation in bacterial cell walls, is also a determinant of antimicrobial activity of Ag NPs on Gram-negative bacteria; in such cells, Ag NPs were found to accumulate in the membrane, significantly increasing membrane permeability and resulting in cell death [2]. Those studies may not adequately account for the antimicrobial mechanism of positively charged Ag NPs, as only Ag^+ ions and negatively charged Ag NPs were tested.

Metal depletion in *E. coli*, which causes a loss of lipopolysaccharide molecules and membrane proteins, leads to the formation of irregularly shaped pits in the outer membrane. Such membranes have higher permeability than cells devoid of this stress [3]. In case of treatment with Ag NPs, disruption of the membrane structure of *E. coli* may follow a similar path. Although it is assumed that Ag NPs are involved in some sort of binding mechanism, the mechanism of the interaction between Ag NPs and components of the outer membrane is still unclear [2]. In a study on multidrug resistant bacteria it was shown, using a sensitivity test (Kirby-Baeur), that both Ag NPs and antibiotics may inhibit cellular processes of cell wall, protein and nucleic acid synthesis [11]. Proteomic analyses of *E. coli* cells exposed to Ag NPs and Ag^+ ions detected increased concentration of precursors of envelop proteins, which indicate a loss of proton motive force [12]. Bactericidal action of Ag^+ were shown to result from a collapse of transmembrane pH and electric potential [13]. Though both Ag NPs and Ag^+ ions have identical effect on the membrane potential, yet Ag NPs are more efficient as their effective concentration is at nanomolar levels compared to micromolar for Ag^+ [12].

More results in *E. coli* suggested that Ag NPs may damage the structure of bacterial cell membranes and depress the activity of some membranous enzymes, which causes the bacteria to die eventually [14].

As it is evident from the above discussion, it is unlikely that the Ag NP-mediated inhibition of microorganisms involves a simple, one-dimensional route. The analysis of intercellular metabolites and gene expression levels could provide information regarding the effect of nanoparticles on the organism as well as the possible causes thereof.

While genomic responses to environmental stress [15] and mechanisms of metal homeostasis and tolerance [16] have been well examined in *Saccharomyces cerevisiae*, information on

A. Haloi is with the Sophisticated Analytical Instrument Facility, North-Eastern Hill University, Shillong 793022, India (e-mail: anjalihaloi@gmail.com)

D. Das was with Dept. of Biotechnology, Gauhati University, Guwahati 781014, India (corresponding author, e-mail: debabrata.gauniv@gmail.com)

molecular responses to nanoparticles are scarce. A recent study described the transcriptome profile of *S. cerevisiae* grown in sublethal amounts of Ag NPs using RNAseq [17]. 'Hundreds of genes in AgNP-treated cells were found to be differentially expressed, including genes implicated in rRNA processing, ribosome biogenesis, cell wall formation, cell membrane integrity and mitochondrial functions' [17].

Here, we assessed the expression levels of two genes involved in rRNA processing and ribosome assembly – *KRR1* and *PWP2* – in *S. cerevisiae* exposed to Ag NPs. The choice of genes was primarily based on an observation of intercellular levels of RNA and proteins in nanoparticle stressed cells.

II. Materials and Methods

A. Synthesis and Characterization of Ag NPs

Ag NPs were synthesized in-house with the Creighton method which involves the reduction of $AgNO_3$ (Sigma-Aldrich) by $NaBH_4$ (Merck). The reactions were carried out in de-ionized water as well as in liquid yeast malt (YM) growth media.

The synthesized Ag NPs were studied for surface plasmon resonance by UV-vis spectrum analysis for constitution and particle size by XRD, and for morphology and size by TEM [18].

B. Test Organism and Growth Conditions

The yeast, *Saccharomyces cerevisiae* (MTCC 36), used in this study, was procured from the Microbial Type Culture Collection & Gene Bank, Institute of Microbial Technology, Chandigarh, India as an active culture on slant. The cells were grown on YM (HiMedia Labs) agar slants at 30 ºC with an incubation time of 48 h. The cultures were then transferred and maintained at refrigerated temperatures and routinely sub-cultured at 30-day intervals. The strain MTCC 36 (equivalent to NRRLY–11857, ATCC26602, and NCYC975) was originally isolated from a sugar refinery.

The MIC and minimum killing concentration (MKC) of Ag NPs against *S. cerevisiae* was determined as by [19]. The yeast cells (~10^6 CFU/ml) were grown in the presence of 5.39, 26.95, 48.51, 64.68, and 70.07 µg/ml of pre-formed Ag NPs in YM media for 36 h in a shaker incubator set at 30 °C/150 rpm. Growth was verified by recording the change in the turbidity of the culture. The lowest concentration of Ag NPs, at which no visual turbidity could be observed, represented the MIC of Ag NPs. The cultures that lacked turbidity were plated onto YM agar. The minimal concentration of Ag NPs where the CFU/ml was < 0.1% of the initial concentration of yeast was taken to represent the MKC. To compare the antimicrobial activity of Ag NPs and Ag^+ ions, the susceptibility constants or Z values of Ag materials were calculated according to:

$$Z = -ln(N/N_0)/C \quad (1)$$

where, N is the number of colony-forming units (CFU) following exposure to Ag material; N_0 is the number of CFUs in the absence of Ag materials; and C is the concentration of Ag material (ppm or µg/ml) [20]. This comparison of the antimicrobial efficacy of Ag NPs and Ag^+ ions was done to preclude the possibility that the effect observed on yeast cells as a result of exposure to the nanoparticle solutions might be influenced by any residual Ag^+ ions present therein.

C. Expression Studies

Nanoparticles with the concentrations described above were synthesized in YM media. A flask containing YM media without Ag NPs was kept as a control. Growth was initiated with 100 µl of a log phase culture (~1.5 x 10^8 CFU/ml). The flasks were then incubated overnight at 30 ºC/120 rpm. These cultures were used for the determination of cellular RNA and protein in cells grown at different Ag NP concentrations. The total protein content was determined by Lowry's method using a kit (GeNei, India) and total cellular RNA levels were determined as described by [21].

For gene expression studies, total RNA was prepared from yeast cultures (~10^7 cells) with a GeneiPure total RNA isolation kit-Yeast (GeNei, India). Reverse transcription was carried out using a first strand cDNA synthesis kit (Fermentas, EU) with oligo-dT (18) primers according to the manufacturer's instructions. RT-PCR reactions were performed on a CFX 95 instrument (Bio-Rad, USA), using an iQ™ SYBR green supermix (Bio-Rad, USA). The amplification reactions were set as follows: 10 min at 95 ºC and 50 cycles at 95 ºC for 15 s, 53 ºC/55 ºC for 35 s and 72 ºC for 45 s. To confirm the primer specificity, the dissociation curves of all amplification products were analyzed. Fold variation in gene expression was quantified using the ΔΔC(t) method. As a reference gene, actin RNA, amplified by *ACT1*, was used to normalize all values in the RT-PCR assays. The primers *KRR1* (forward: 5′-AGG AAT GTG GCC AGA AAG AA-3′; reverse: 5′-TTC CTG CCT TTC GAT TTC TC-3′), *PWP2* (forward: 5′- TGT AAG CAA AGA CGG TGC TG-3′; reverse: 5′- AAA AGC CTT GTT GCT GGA TG-3′), and *ACT1* (forward: 5′- CGT TCC AAT TTA CGC TGG TT-3′; reverse: 5′- AGC GGT TTG CAT TTC TTG TT-3′) used for amplification were designed with the Primer3 software (http://biotools.umassmed.edu/bioapps/primer3_www.cgi) using coding sequences sourced from the Saccharomyces Genome Database (www.yeastgenome.org). The primers were 'tested' using the BLASTn sequence alignment algorithm (http://blast.ncbi.nlm.nih.gov/ Blast.cgi); primers were deemed suitable if they would not bind to a template other than the one of interest. These primers comprised 20 nucleotides with 40–60% GC contents, and the target amplicon length was between 155 and 206 bp. All primers were designed with the procedure described above and purchased from Metabion, Germany.

III. Results and Discussion

A. Synthesis and Characterization

Ag NPs were readily synthesized in YM media without the use of any additional stabilizing agents. Electron micrographs show the presence of well dispersed particles with a smooth spherical morphology and a mean size of 8.6 nm. The size distribution was narrow ranging from 2.5 nm to > 50 nm (Fig. 1).

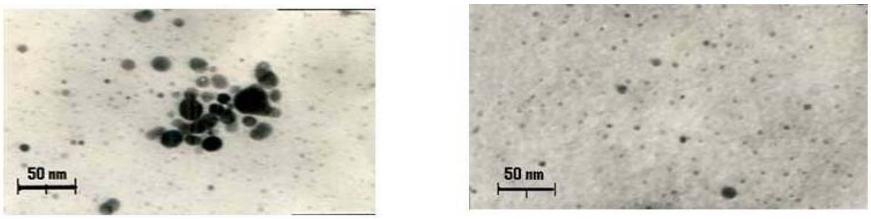

Fig. 1 TEM images of synthesized Ag NPs

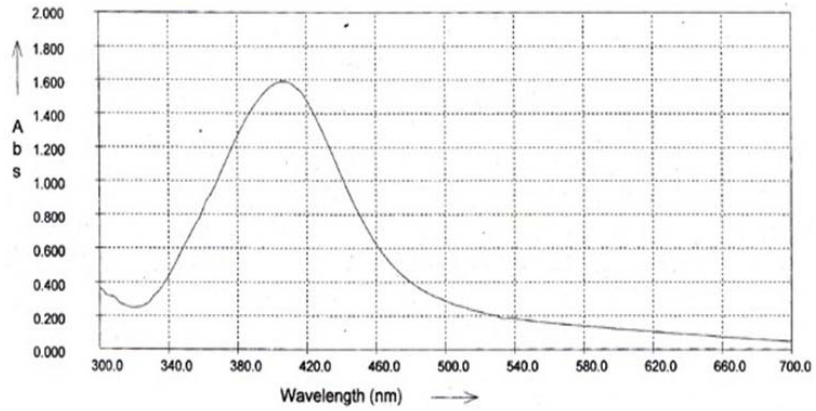

UV-Vis spectra of Ag NP (26.95 µg/ml): peak absorption at 407.0 nm

Optical characteristics

Ag NP solutions (µg/ml)	λ_{max} (nm)	FWHM (nm)
5.39	416.5	77.50
26.95	407.0	92.50
48.51	392.0	108.75
64.68	390.5	93.75
70.07	393.5	85.00

Fig. 2 UV-VIS absorption spectra of Ag NP solutions

The individual UV-VIS absorption spectra of the Ag NP samples, with particle concentrations of 5.39 µg/ml to 70.07 µg/ml, show smooth absorption bands with a single pronounced plasmon resonance around 400 nm (Fig. 2). Electronic transitions involving the Ag^+ ion give rise to absorption bands located between 200 and 230 nm, whereas the electronic transitions of metallic Ag^0 appear in the 250-330 nm spectral range [22]. The UV-VIS spectra of all samples analyzed in this study did not show any distinct absorption signals around 230 nm arising from the electronic transitions involving Ag^+ ions. Moreover, a large excess of the reducing agent was used during the synthesis process, possibly leading to a complete reduction of the Ag salt. The presence of Ag^+ ions in the synthesized nanoparticle solutions can thus be safely assumed to be either nonexistent or of infinitesimal concentration. A comparison of the full-width at half maximum (FWHM) values obtained for the different particle solutions (Fig. 2) confirms the formation of nanoparticles with uniform size distribution. When the solution system is monodisperse (narrow size distribution), the peak shape is symmetric and the value of the FWHM is small. When the system is polydisperse, the peak shape is asymmetric, which suggests that the peak actually consists of two or more absorption peaks [23]. We found that the peak shapes were symmetric, and the corresponding FWHM values ranged from 108 to 77 nm. These results imply that the size distribution became narrower, and the colloid system was monodisperse. The analysis of the electron micrographs of the synthesized nanoparticles largely confirms the results obtained from UV-Vis spectra.

The XRD pattern of the synthesized nanoparticles (Fig. 3) showed diffraction peaks at $2\theta = 38.3^o$, 44.5^o, 64.6^o, and 77.1^o, which can be respectively indexed to the (111), (200), (220), and (311) planes of pure silver. These data correlate well with the powder diffraction file (PDF) no. 04-0783 pertaining to pure Ag, available from the Joint Committee on Powder Diffraction Standards (JCPDS). The results indicate the presence of Ag in the form of highly crystalline face-centered cubic (FCC) structures of Ag NPs [24], [25]. It may be noted that an additional peak at $2\theta = 81.5^o$ (approximately) has been observed, corresponding to the (222) lattice plane [26], [27]. In the current study, this peak index is missing as the diffracted intensities were recorded only up to angles of 79.9^o 2θ. The particle size calculated from the high intensity (111) peak was 10.3 nm and the corresponding crystallinity index (I_{cry}) was

0.83. If crystallinity (I_{cry}) is close to 1, then it is assumed that the crystallite size represents monocrystalline units whereas a polycrystalline population would have a much larger crystallinity index [27].

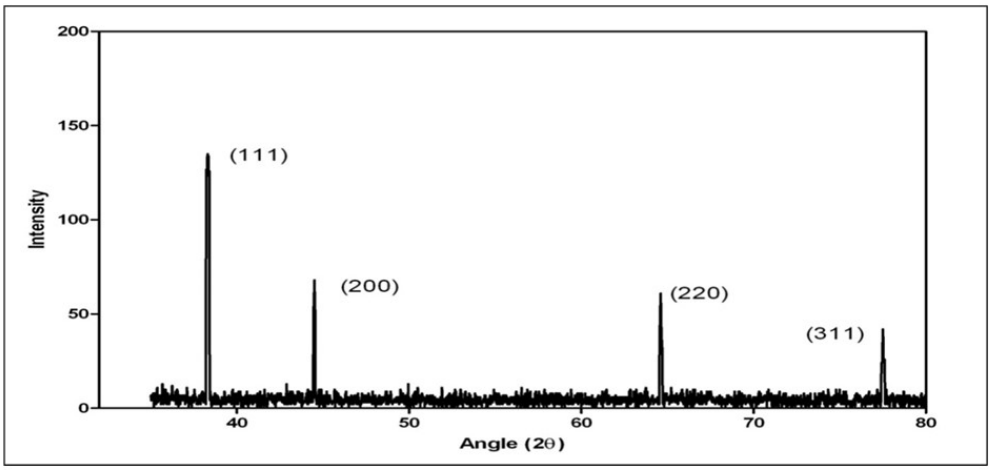

XRD spectra of Ag NP (26.95 µg/ml): peak indices and 2θ positions

Particle size

Particle concentration	2θ (degree)	FWHM (radian)	Particle size (nm)	Crystal lattice
26.95 µg/ml	38.31	0.014	10.3	fcc
70.07 µg/ml	38.35	0.013	10.9	fcc

Crystallinity index

Sample	D_p (nm)	D_{cry} (nm)	I_{cry}	Particle Type
Silver Nanoparticles	8.6	10.3	0.83	Monocrystalline

Fig. 3 XRD spectra: The crystalline size was calculated from the half-height width of diffraction peaks using the Debye-Scherrer equation

A similar synthesis process reported particle sizes ranging from 2 to 5 nm [19]. Kim et al. reported the synthesis of highly monodisperse particles with an average diameter of 13.5 nm [10]. In their study, the synthesis was accomplished in triple distilled water without additional stabilizers. However, Ag NPs have been synthesized using stabilizing agents such as Daxad 19 and ascorbic acid as the reducing agent, with a mean particle size of 12.3 nm [2]. Apart from the use of stabilizers, size is also influenced by the choice and concentration of the reducing agent used for synthesis. The antimicrobial properties of Ag NPs are size-dependent as smaller-sized particles possess a larger surface area to volume ratio. In our study, the particle size obtained was similar to that of previous reports [19], [10], [2] and could be expected to influence the growth and cellular activities of the test organism.

B. Inhibitory Concentrations

To determine the MIC, it was observed that the lowest concentration of Ag NPs at which no visible turbidity was observed, and which recorded a transmission of 100% was 48.51 µg/ml. This value was taken as the MIC of Ag NPs for *S. cerevisiae*. Each of the non-turbid cultures (with concentrations of 48.45 µg/ml and more) was then plated onto YM agar and the number of colonies was counted. It was observed that the growth of cells in the presence of 70.07 µg/ml of nanoparticles led to a decrease of > 99% of the initial cell concentration. According to the criterion that the MKC had a minimum concentration of Ag NPs where the CFU/ml was < 0.1% of the initial concentration, we concluded that 70.07 µg/ml was the MKC of Ag NPs for *S. cerevisiae*. Inhibitory concentrations were dependent on the species tested and the method employed. The MIC values of > 6.6 nM against yeast (ATCC19636) [10] and of 0.42 mg/L against *Candida albicans* [28] are lower than those found in the current study. In addition, significantly higher values of MIC50 of 0.5 mg/ml and 4 mg/ml have been reported in *Candida albicans* (ATCC 5027) and *Saccharomyces cerevisiae* (ATCC 5027), respectively [29]. The use of stabilizing agents in particle synthesis also contributes towards inhibition, however, in the present study this was avoided by directly synthesizing nanoparticles in growth media without the use of stabilizers. The MKC value of 70.07 µg/ml provided an upper limit of treatment in experiments concerning metabolic and gene expression studies.

To compare the antimicrobial effect of any residual Ag^+ ions that might be present in the nanoparticle preparations, we determined the susceptibility constants or Z values of equivalent concentrations of Ag NPs and Ag^+ ions ($AgNO_3$). At a given concentration, the susceptibility constants were higher for Ag NPs than those of Ag^+ ions (Fig. 2). The corresponding values obtained at the MIC (48.51 µg/ml) and MKC (70.07 µg/ml) doses were significantly higher in the case of nanoparticles being 0.0413 (Ag NPs) against 0.0080 (ions) and 0.1045 (Ag NPs) against 0.0522 (ions), respectively. A higher Z value implies that the microbes are more sensitive to the material, indicating that the materials are more toxic to the microbes [20]. A larger excess of the reducing agent $NaBH_4$ (up to 2 x 10^2 times) than that of the silver salt (Ag NO_3) was used during the preparation of the nanoparticles. Under the synthesis conditions employed, all the Ag salt was reduced and any proportion of Ag^+ ions left was negligible. The effect on the

yeast cells arising due to exposure to Ag NPs in YM media was likely due to nanoparticles alone. As it is evident from the comparison of the antimicrobial effects of Ag NPs and ions of equivalent concentrations, the presence of any residual ions left-over from the synthesis process would not influence the effect of Ag NPs on yeast cells. In all subsequent experiments of this study, the effect of Ag NPs alone was considered as it was evident that the test solutions were composed almost entirely of nanoparticles and also, as discussed in the findings above, Ag NPs have a more potent effect on yeast cells than Ag^+ ions of equivalent concentrations.

C. Expression Studies

The intracellular metabolite concentrations were investigated to assess the impact of nanoparticles on the metabolic activities of yeast cells. Baker's yeast cells may change their level of metabolic activity, such as their carbon metabolism and nitrogen metabolism, as well as their stress response to environmental conditions [30]. The cellular metabolite levels in yeast cells were clearly influenced by the presence of nanoparticles in the growth medium. The cellular protein concentrations of stressed cells showed a steady decrease when cells were exposed to increasingly higher doses of Ag NPs. The total RNA levels, however, were relatively consistent at nanoparticle concentrations below the lethal dose and then showed a substantial reduction at the MIC concentration and beyond (Fig. 4). This observation seems to predict that in nanoparticle stressed cells which are yet viable, some aspects of metabolism related to protein synthesis are inhibited leading to a state where RNA levels are normal, but protein contents have decreased. Environmental stress, including exposure to heavy metals, affects functioning of cellular processes carried out by large macromolecular complexes. As protein synthesis involves several such macromolecular complexes, the process is sensitive to external stress [31].

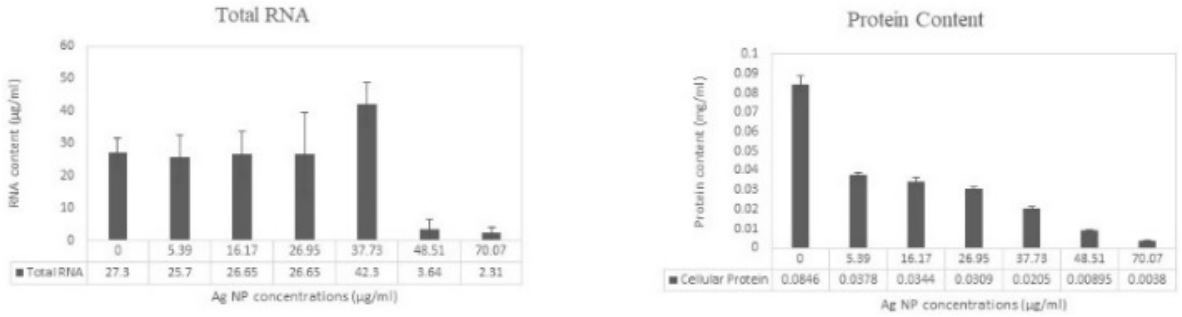

Fig. 4 Total RNA/protein in Ag NP stressed cells

Previous genome-wide studies [32] of yeasts exposed to heavy metal stress have indicated a decreased expression of genes involved in ribosome biogenesis and assembly. In the current study, we assessed the expression levels of two genes involved in rRNA processing and ribosome assembly – *KRR1* and *PWP2* – in *S. cerevisiae* exposed to Ag NPs. *KRR1* is an essential nucleolar protein required for the synthesis of 18S rRNA and for the assembly of 40S ribosomal subunits, while *PWP2* encodes a conserved 90S pre-ribosomal component essential for the proper endonucleolytic cleavage of the 35S rRNA precursor (http://yeastgenome.org). Importantly, these genes have functional homologues in humans.

The expressions of the two rRNA maturation genes assessed in this study were found to be downregulated in nanoparticle stressed cells (Table I & Fig. 5). At the MKC of 70.07 µg/ml there was an up to 260-fold decrease in transcript levels for *KRR1* and a 42-fold decrease for *PWP2* compared to that of the control cells. The decrease in the mRNA quantity at the MIC of 48.51 µg/ml was found to be 90-fold for *KRR1* and ~7-fold for *PWP2*. Differences in expression for cells grown in media with 48.51 µg/ml and 70.07 µg/ml nanoparticle concentrations were found to be statistically significant ($p < 0.05$). Cells grown at the sub-lethal nanoparticle concentration of 26.95 µg/ml were also found to contain lower mRNA levels of both the assayed genes. However, the differences in expression were not statistically significant.

TABLE I
FOLD-VARIATIONS AND UN-PAIRED T-TEST OF MRNA LEVELS IN NANOPARTICLE STRESSED CELLS WITH REGARD TO CONTROL

Ag NP Conc^n (µg/ml)	*KRR1*		*PWP2*	
	Fold variation	*p* value	Fold variation	*p* value
26.95	- 3.0	0.299	- 2.0	0.119
48.51	- 9.0 x 10	0.045*	- 7.1	0.039*
70.07	- 2.6 x 10^2	0.044*	- 4.2 x 10	0.031*

* significant

A recent study analyzed the transcriptome profile of *S. cerevisiae* using RNAseq data [17]. Interestingly, more than 80 out of 144 of the most upregulated genes subjected to a 5 µg/mL (sub-lethal) treatment of AgNPs were identified to function for rRNA processing/ribosome biogenesis. Many of the translated products of these 80 genes are located in the nucleolus and associated with rRNA processing/ribosome biogenesis, including *KRR1* and *PWP2*. These data appear to differ from the findings of the present study. However, it may be important to consider that Ag NP concentration employed was significantly different, and the RNAseq data of only four genes were validated with qRT-PCR which did not include *KRR1* or *PWP2*. The authors conjecture that 'AgNPs appear to affect the integrity of ribosomes, which might end up elevating the expression levels of genes implicated in rRNA processing and the biogenesis of small large subunit ribosomes as well as the

nuclear export of ribosomes' [17].

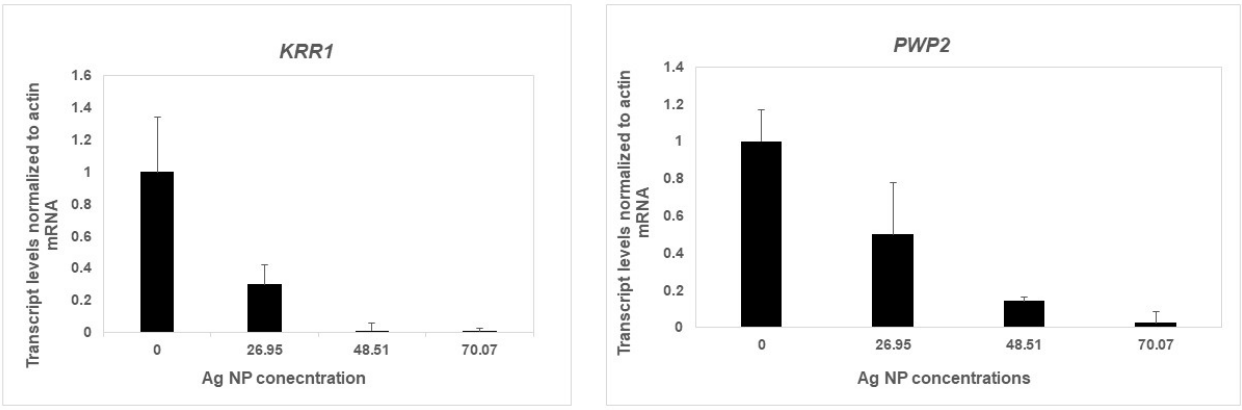

Fig. 5 Fold variations of *KRR1* & *PWP2* in Ag NP stressed cells compared to cells grown in YM media alone

Global gene responses in *S. cerevisiae* showed that Ag NPs induced a differential expression of genes involved in metabolism and transcription categories, among others [33]. Silver ions, more than Ag NPs, were found to repress genes involved in protein synthesis. In a study on the genomic effects of exposure to transition metals on *S. cerevisiae* [32], it was reported that the genes involved in ribosome biogenesis and assembly were repressed when cells were exposed to 10μM and 20 μM concentrations of silver. The authors identified, using Cytoscape, the metal-responsive protein-protein and protein-DNA interacting networks and reported *PWP2* and *KRR1* amongst the ten most significant sub-networks regulated by silver. Ribosome production may represent over 50% of the synthetic effort involved in rapidly growing eukaryotic cells [15]. Therefore, by inhibiting ribosome synthesis, cells may be able to redirect these resources towards their defense against metal toxicity [34], [35]. The present study indicates that on exposure to Ag NPs, *KRR1* and *PWP2*, genes related to rRNA biogenesis and processing, are repressed. Further studies could investigate whether (or not) Ag NPs cause a disruption of ribosomal assembly and function in yeasts.

REFERENCES

[1] H.H. Lara, E.N. Garza-Treviño, L. Ixtepan-Turrent, and D.K. Singh, "Silver nanoparticles are broad-spectrum bactericidal and virucidal compounds," *J Nanobiotechnol*, vol. 9, Aug. 2011.

[2] I. Sondi, and B. Salopek-Sondi, "Silver nanoparticles as antimicrobial agent: A case study on *E. coli* as a model for Gram-negative bacteria," *J Colloid Interface Sci*, vol. 275, no. 1, pp. 177-182, Jul. 2004.

[3] N.A. Amro, L.P. Kotra, K. Wadu-Mesthrige, A. Bulychev, S. Mobashery, and G. Liu, "High-resolution atomic force microscopy studies of the *Escherichia coli* outer membrane: structural basis for permeability," *Langmuir*, vol. 16, no. 6, pp. 2789-2796, Jan. 2000.

[4] P.K. Stoimenov, R.L. Klinger, G.L. Marchin, and K.J. Klabunde, "Metal oxide nanoparticles as bactericidal agents," *Langmuir*, vol. 18, no. 17, pp. 6679-6686, Jul. 2002.

[5] Q.L. Feng, J. Wu, G.Q. Chen, F.Z. Cui, T.M. Kim, and J.O. Kim, "A mechanistic study of the antibacterial effect of silver ions on Escherichia coli and Staphylococcus aureus," *J Biomed Mater Res*, vo. 52, no. 4, pp. 662-668, Dec. 2000.

[6] J.R. Morones, J.L. Elechiguerra, A. Camacho, K. Holt, J.B. Kouri, J.T. Ramırez, and M.J. Yacaman, "The bactericidal effect of silver nanoparticles," *Nanotechnology*, vol. 16, no. 10, pp. 2346-2353, Oct. 2005.

[7] S. Pal, Y.K. Tak, and J.M. Song, "Does the Antibacterial Activity of Silver Nanoparticles Depend on the Shape of the Nanoparticle? A Study of the Gram-Negative Bacterium Escherichia coli," *Appl Environ Microbiol*, vol. 73, no. 6, pp. 1712-1720, Mar. 2007.

[8] H.J. Yen, S.H. Hsu, and C.L. Tsai, "Cytotoxicity and immunological response of gold and silver nanoparticles of different sizes," *Small*, vol. 5, no. 13, pp. 1553-1561, Jul. 2009.

[9] J.P. Ruparelia, A.K. Chatterjee, S.P. Duttagupta, and S. Mukherji, "Strain specificity in antimicrobial activity of silver and copper nanoparticles," *Acta Biomater*, vol. 4, no. 3, pp. 707-716, May 2008.

[10] J.S. Kim, E. Kuk, K.N. Yu, J.H. Kim, S.J. Park, H.J. Lee, S.H. Kim, Y.K. Park, Y.H. Park, C.Y. Hwang, Y.K. Kim, Y.S. Lee, D.H. Jeong, and M.H. Cho, "Antimicrobial effects of silver nanoparticles," *Nanomedicine*, vol. 3, no. 1, pp. 95-101, Mar. 2007.

[11] H.H. Lara, N.V. Ayala-Nuñez, L. Ixtepan-Turrent, and C. Rodriguez-Padilla, "Bactericidal effect of silver nanoparticles against multidrug-resistant bacteria," *World J Microbiol Biotechnol*, vol. 26, pp. 615-621, Apr. 2010.

[12] C.N. Lok, C.M. Ho, R. Chen, Q.Y. He, W.Y. Yu, H. Sun, P.K. Tam, J.F. Chiu, and C.M. Che, "Proteomic analysis of the mode of antibacterial action of silver nanoparticles," *J Proteome Res*, vol. 5, no. 4, pp. 916-924, Mar. 2006.

[13] P. Dibrov, J. Dzioba, K.K. Gosink, and C.C. Hase, "Chemiosmotic mechanism of antimicrobial activity of Ag(+) in *Vibrio cholerae*," *Antimicrob Agents Chemother*, vol. 46, no. 8, pp. 2668-2670, Aug. 2002.

[14] W.R. Li, X.B. Xie, Q.S. Shi, H.Y. Zeng, Y.S. Ou-Yang and Y.B. Chen, "Antibacterial activity and mechanism of silver nanoparticles on *Escherichia coli*," *Appl Microbiol Biotechnol*, vol. 85, pp. 1115-1122, Jan. 2010.

[15] A.P. Gasch, P.T. Spellman, C.M. Kao, O. Carmel-Harel, M.B. Eisen, G. Storz, D. Botstein, and P.O. Brown, "Genomic expression programs in the response of yeast cells to environmental changes," *Mol Biol Cell*, vol. 11, no. 12, pp. 4241-4257, Dec. 2000.

[16] M.J. Tamas, J. Labarre, M.B. Toledano, and R. Wysocki, "*Mechanisms of toxic metal tolerance in yeast*," in *Molecular biology of metal homeostasis and detoxification: from microbes to man*, M.J. Tamás, and E. Martinoia, Eds. Heidelberg: Springer, 2005, pp. 395-454.

[17] C. Horstmann, C. Campbell, D.S. Kim, and K. Kim, "Transcriptome profile with 20 nm silver nanoparticles in yeast," FEMS *Yeast Res*, vol. 19, no. 2, foz003, Mar. 2019.

[18] D. Das, and G.U. Ahmed, "Cellular Responses of *Saccharomyces cerevisiae* to silver nanoparticles," *Res J BioTechnol*, vol. 8, no. 1, pp. 72-77, Jan. 2013.

[19] S.K. Gogoi, P. Gopinath, A. Paul, A. Ramesh, S.S. Ghosh, and A. Chattopadhyay, "Green Fluorescent Protein-Expressing *Escherichia coli* as a Model System for Investigating the Antimicrobial Activities of Silver Nanoparticles," *Langmuir*, vol. 22, no. 22, pp. 9322-9328, Oct. 2006.

[20] S. Lee, J. Lee, K. Kim, S-J. Sim, M.B. Gu, J. Yi, and J. Lee, "Ecotoxicity of Commercial Silver Nanopowders to Bacterial and Yeast Strains," *Biotechnol Bioprocess Eng,* vol. 14, pp. 490-495 Sep. 2009.

[21] S. Benthin, J. Nielsen, and J. Villadsen, "A simple and reliable method for the determination of cellular RNA content," *Biotechnol Tech,* vol. 5,

pp. 39-42, Jan. 1991.
[22] J. Lu, J.J. Bravo-Suárez, A. Takahashi, M. Haruta, and S.T. Oyama, "In situ UV–vis studies of the effect of particle size on the epoxidation of ethylene and propylene on supported silver catalysts with molecular oxygen," *J Catal*, vol. 232, no. 1, pp. 85-95, May 2005.
[23] K.R. Brown, D.G. Walter, and M.J. Natan, "Seeding of Colloidal Au Nanoparticle Solutions. 2. Improved Control of Particle Size and Shape," *Chem Mater*, vol. 12, no. 2, pp. 306-313, Feb. 2000.
[24] X. Wang, J. Zhuang, Q. Peng, and Y. Li, "A general strategy for nanocrystal synthesis," *Nature*, vol. 437, pp. 121-124, Sep. 2005.
[25] A.S. Lanje, S.J. Sharma, and R.B. Pode, "Synthesis of silver nanoparticles: a safer alternative to conventional antimicrobial and antibacterial agents," *J Chem Pharm Res*, vol. 2, no. 2, pp. 478-483, Mar. 2010.
[26] C. Liu, X. Yang, H. Yuan, Z. Zhou, and D. Xiao, "Preparation of Silver Nanoparticle and Its Application to the Determination of *ct*-DNA," *Sensors*, vol. 7, no. 5, pp. 708-718, May 2007.
[27] X. Pan, I. Medina-Ramirez, R. Mernaugh, and J. Liu, "Nanocharacterization and bactericidal performance of silver modified titania photocatalyst," *Colloids Surf B*, vol. 77, no. 1, pp. 82-89, May 2010.
[28] A. Panacek, M. Kolar, R. Vecerova, R. Prucek, J. Soukupova, V. Krystof, P. Hamal, R. Zboril, and L.Kvıtek, "Antifungal activity of silver nanoparticles against *Candida spp*.," *Biomaterials*, vol. 30, no. 31, pp. 6333-63340, Oct. 2009.
[29] A. Nasrollahi, K. Pourshamsian, and P. Mansourkiaee, "Antifungal activity of silver nanoparticles on some of fungi," *Int J Nano Dimens,* vol. 1, no. 3, pp. 233-239, Winter 2011
[30] V.J. Higgins, P.J. Bell, I.W. Dawes, and P.V. Attfield, "Generation of a Novel *Saccharomyces cerevisiae* Strain That Exhibits Strong Maltose Utilization and Hyperosmotic Resistance Using Nonrecombinant Techniques," *Appl Environ Microbiol*, vol. 67, no. 9, pp. 4346-4348, Sep. 2001.
[31] U. Bond, "Stressed out! Effects of environmental stress on mRNA metabolism," *FEMS Yeast Res*, vol. 6, no. 2, pp. 160-170, Mar. 2006.
[32] Y.H. Jin, P.E. Dunlap, S.J. McBride, H. Al-Refai, P.R. Bushel, and J.H. Freedman, "Global transcriptome and deletome profiles of yeast exposed to transition metals," *PLoS Genet*, vol. 4, no. 4, pp. e1000053, Apr. 2008.
[33] J.H. Niazi, B-I. Sang, Y.S. Kim, and M.B. Gu, "Global Gene Response in Saccharomyces cerevisiae Exposed to Silver Nanoparticles," *Appl Biochem Biotechnol*, vol. 164, pp. 1278-1291, Mar. 2011.
[34] M.J. Miller, N.H. Xuong, and E.P. Geiduschek, "Quantitative analysis of the heat shock response of *Saccharomyces cerevisiae*," *J Bacteriol*, vol. 151, no. 1, pp. 311-327, Jul. 1982.
[35] T. Moss, "At the crossroads of growth control; making ribosomal RNA," *Curr Opin Genet Dev*, vol. 14, no. 2, pp. 210-217, Apr. 2004.